RAPID COMMUNICATIONS

PHYSICAL REVIEW D **83,** 031105(R) (2011)

Measurement of the ratio of inclusive cross sections $\sigma(p\bar{p} \to Z + b\text{-quark jet})/\sigma(p\bar{p} \to Z + \text{jet})$ at $\sqrt{s} = 1.96$ TeV

V. M. Abazov,[35] B. Abbott,[72] B. S. Acharya,[29] M. Adams,[48] T. Adams,[46] G. D. Alexeev,[35] G. Alkhazov,[39] A. Alton,[60,*]
G. Alverson,[59] G. A. Alves,[2] L. S. Ancu,[34] M. Aoki,[47] Y. Arnoud,[14] M. Arov,[57] A. Askew,[46] B. Åsman,[40] O. Atramentov,[64]
C. Avila,[8] J. BackusMayes,[79] F. Badaud,[13] L. Bagby,[47] B. Baldin,[47] D. V. Bandurin,[46] S. Banerjee,[29] E. Barberis,[59]
P. Baringer,[55] J. Barreto,[2] J. F. Bartlett,[47] U. Bassler,[18] V. Bazterra,[48] S. Beale,[6] A. Bean,[55] M. Begalli,[3] M. Begel,[70]
C. Belanger-Champagne,[40] L. Bellantoni,[47] S. B. Beri,[27] G. Bernardi,[17] R. Bernhard,[22] I. Bertram,[41] M. Besançon,[18]
R. Beuselinck,[42] V. A. Bezzubov,[38] P. C. Bhat,[47] V. Bhatnagar,[27] G. Blazey,[49] S. Blessing,[46] K. Bloom,[63] A. Boehnlein,[47]
D. Boline,[69] T. A. Bolton,[56] E. E. Boos,[37] G. Borissov,[41] T. Bose,[58] A. Brandt,[75] O. Brandt,[23] R. Brock,[61] G. Brooijmans,[67]
A. Bross,[47] D. Brown,[17] J. Brown,[17] X. B. Bu,[47] M. Buehler,[78] V. Buescher,[24] V. Bunichev,[37] S. Burdin,[41,†] T. H. Burnett,[79]
C. P. Buszello,[40] B. Calpas,[15] E. Camacho-Pérez,[32] M. A. Carrasco-Lizarraga,[55] B. C. K. Casey,[47] H. Castilla-Valdez,[32]
S. Chakrabarti,[69] D. Chakraborty,[49] K. M. Chan,[53] A. Chandra,[77] G. Chen,[55] S. Chevalier-Théry,[18] D. K. Cho,[74]
S. W. Cho,[31] S. Choi,[31] B. Choudhary,[28] T. Christoudias,[42] S. Cihangir,[47] D. Claes,[63] J. Clutter,[55] M. Cooke,[47]
W. E. Cooper,[47] M. Corcoran,[77] F. Couderc,[18] M.-C. Cousinou,[15] A. Croc,[18] D. Cutts,[74] M. Ćwiok,[30] A. Das,[44]
G. Davies,[42] K. De,[75] S. J. de Jong,[34] E. De La Cruz-Burelo,[32] F. Déliot,[18] M. Demarteau,[47] R. Demina,[68] D. Denisov,[47]
S. P. Denisov,[38] S. Desai,[47] K. DeVaughan,[63] H. T. Diehl,[47] M. Diesburg,[47] A. Dominguez,[63] T. Dorland,[79] A. Dubey,[28]
L. V. Dudko,[37] D. Duggan,[64] A. Duperrin,[15] S. Dutt,[27] A. Dyshkant,[49] M. Eads,[63] D. Edmunds,[61] J. Ellison,[45]
V. D. Elvira,[47] Y. Enari,[17] H. Evans,[51] A. Evdokimov,[70] V. N. Evdokimov,[38] G. Facini,[59] T. Ferbel,[68] F. Fiedler,[24]
F. Filthaut,[34] W. Fisher,[61] H. E. Fisk,[47] M. Fortner,[49] H. Fox,[41] S. Fuess,[47] T. Gadfort,[70] A. Garcia-Bellido,[68] V. Gavrilov,[36]
P. Gay,[13] W. Geist,[19] W. Geng,[15,61] D. Gerbaudo,[65] C. E. Gerber,[48] Y. Gershtein,[64] G. Ginther,[47,68] G. Golovanov,[35]
A. Goussiou,[79] P. D. Grannis,[69] S. Greder,[19] H. Greenlee,[47] Z. D. Greenwood,[57] E. M. Gregores,[4] G. Grenier,[20] Ph. Gris,[13]
J.-F. Grivaz,[16] A. Grohsjean,[18] S. Grünendahl,[47] M. W. Grünewald,[30] F. Guo,[69] G. Gutierrez,[47] P. Gutierrez,[72] A. Haas,[67,‡]
S. Hagopian,[46] J. Haley,[59] L. Han,[7] K. Harder,[43] A. Harel,[68] J. M. Hauptman,[54] J. Hays,[42] T. Head,[43] T. Hebbeker,[21]
D. Hedin,[49] H. Hegab,[73] A. P. Heinson,[45] U. Heintz,[74] C. Hensel,[23] I. Heredia-De La Cruz,[32] K. Herner,[60] G. Hesketh,[59]
M. D. Hildreth,[53] R. Hirosky,[78] T. Hoang,[46] J. D. Hobbs,[69] B. Hoeneisen,[12] M. Hohlfeld,[24] S. Hossain,[72] Z. Hubacek,[10,18]
N. Huske,[17] V. Hynek,[10] I. Iashvili,[66] R. Illingworth,[47] A. S. Ito,[47] S. Jabeen,[74] M. Jaffré,[16] S. Jain,[66] D. Jamin,[15] R. Jesik,[42]
K. Johns,[44] M. Johnson,[47] D. Johnston,[63] A. Jonckheere,[47] P. Jonsson,[42] J. Joshi,[27] A. Juste,[47,§] K. Kaadze,[56] E. Kajfasz,[15]
D. Karmanov,[37] P. A. Kasper,[47] I. Katsanos,[63] R. Kehoe,[76] S. Kermiche,[15] N. Khalatyan,[47] A. Khanov,[73] A. Kharchilava,[66]
Y. N. Kharzheev,[35] D. Khatidze,[74] M. H. Kirby,[50] J. M. Kohli,[27] A. V. Kozelov,[38] J. Kraus,[61] A. Kumar,[66] A. Kupco,[11]
T. Kurča,[20] V. A. Kuzmin,[37] J. Kvita,[9] S. Lammers,[51] G. Landsberg,[74] P. Lebrun,[20] H. S. Lee,[31] S. W. Lee,[54] W. M. Lee,[47]
J. Lellouch,[17] L. Li,[45] Q. Z. Li,[47] S. M. Lietti,[5] J. K. Lim,[31] D. Lincoln,[47] J. Linnemann,[61] V. V. Lipaev,[38] R. Lipton,[47]
Y. Liu,[7] Z. Liu,[6] A. Lobodenko,[39] M. Lokajicek,[11] P. Love,[41] H. J. Lubatti,[79] R. Luna-Garcia,[32,‖] A. L. Lyon,[47]
A. K. A. Maciel,[2] D. Mackin,[77] R. Madar,[18] R. Magaña-Villalba,[32] S. Malik,[63] V. L. Malyshev,[35] Y. Maravin,[56]
J. Martínez-Ortega,[32] R. McCarthy,[69] C. L. McGivern,[55] M. M. Meijer,[34] A. Melnitchouk,[62] D. Menezes,[49]
P. G. Mercadante,[4] M. Merkin,[37] A. Meyer,[21] J. Meyer,[23] N. K. Mondal,[29] G. S. Muanza,[15] M. Mulhearn,[78] E. Nagy,[15]
M. Naimuddin,[28] M. Narain,[74] R. Nayyar,[28] H. A. Neal,[60] J. P. Negret,[8] P. Neustroev,[39] S. F. Novaes,[5] T. Nunnemann,[25]
G. Obrant,[39] J. Orduna,[32] N. Osman,[42] J. Osta,[53] G. J. Otero y Garzón,[1] M. Owen,[43] M. Padilla,[45] M. Pangilinan,[74]
N. Parashar,[52] V. Parihar,[74] S. K. Park,[31] J. Parsons,[67] R. Partridge,[74,‡] N. Parua,[51] A. Patwa,[70] B. Penning,[47] M. Perfilov,[37]
K. Peters,[43] Y. Peters,[43] G. Petrillo,[68] P. Pétroff,[16] R. Piegaia,[1] J. Piper,[61] M.-A. Pleier,[70] P. L. M. Podesta-Lerma,[32,¶]
V. M. Podstavkov,[47] M.-E. Pol,[2] P. Polozov,[36] A. V. Popov,[38] M. Prewitt,[77] D. Price,[51] S. Protopopescu,[70] J. Qian,[60]
A. Quadt,[23] B. Quinn,[62] M. S. Rangel,[2] K. Ranjan,[28] P. N. Ratoff,[41] I. Razumov,[38] P. Renkel,[76] P. Rich,[43] M. Rijssenbeek,[69]
I. Ripp-Baudot,[19] F. Rizatdinova,[73] M. Rominsky,[47] C. Royon,[18] P. Rubinov,[47] R. Ruchti,[53] G. Safronov,[36] G. Sajot,[14]
A. Sánchez-Hernández,[32] M. P. Sanders,[25] B. Sanghi,[47] A. S. Santos,[5] G. Savage,[47] L. Sawyer,[57] T. Scanlon,[42]
R. D. Schamberger,[69] Y. Scheglov,[39] H. Schellman,[50] T. Schliephake,[26] S. Schlobohm,[79] C. Schwanenberger,[43]
R. Schwienhorst,[61] J. Sekaric,[55] H. Severini,[72] E. Shabalina,[23] V. Shary,[18] A. A. Shchukin,[38] R. K. Shivpuri,[28] V. Simak,[10]
V. Sirotenko,[47] P. Skubic,[72] P. Slattery,[68] D. Smirnov,[53] K. J. Smith,[66] G. R. Snow,[63] J. Snow,[71] S. Snyder,[70]
S. Söldner-Rembold,[43] L. Sonnenschein,[21] A. Sopczak,[41] M. Sosebee,[75] K. Soustruznik,[9] B. Spurlock,[75] J. Stark,[14]
V. Stolin,[36] D. A. Stoyanova,[38] M. Strauss,[72] D. Strom,[48] L. Stutte,[47] L. Suter,[43] P. Svoisky,[72] M. Takahashi,[43]
A. Tanasijczuk,[1] W. Taylor,[6] M. Titov,[18] V. V. Tokmenin,[35] Y.-T. Tsai,[68] D. Tsybychev,[69] B. Tuchming,[18] C. Tully,[65]
P. M. Tuts,[67] L. Uvarov,[39] S. Uvarov,[39] S. Uzunyan,[49] R. Van Kooten,[51] W. M. van Leeuwen,[33] N. Varelas,[48]

E. W. Varnes,[44] I. A. Vasilyev,[38] P. Verdier,[20] L. S. Vertogradov,[35] M. Verzocchi,[47] M. Vesterinen,[43] D. Vilanova,[18]
P. Vint,[42] P. Vokac,[10] H. D. Wahl,[46] M. H. L. S. Wang,[68] J. Warchol,[53] G. Watts,[79] M. Wayne,[53] M. Weber,[47,**]
L. Welty-Rieger,[50] A. White,[75] D. Wicke,[26] M. R. J. Williams,[41] G. W. Wilson,[55] S. J. Wimpenny,[45] M. Wobisch,[57]
D. R. Wood,[59] T. R. Wyatt,[43] Y. Xie,[47] C. Xu,[60] S. Yacoob,[50] R. Yamada,[47] W.-C. Yang,[43] T. Yasuda,[47] Y. A. Yatsunenko,[35]
Z. Ye,[47] H. Yin,[47] K. Yip,[70] S. W. Youn,[47] J. Yu,[75] S. Zelitch,[78] T. Zhao,[79] B. Zhou,[60] J. Zhu,[60] M. Zielinski,[68]
D. Zieminska,[51] and L. Zivkovic[67]

(D0 Collaboration)

[1]*Universidad de Buenos Aires, Buenos Aires, Argentina*
[2]*LAFEX, Centro Brasileiro de Pesquisas Físicas, Rio de Janeiro, Brazil*
[3]*Universidade do Estado do Rio de Janeiro, Rio de Janeiro, Brazil*
[4]*Universidade Federal do ABC, Santo André, Brazil*
[5]*Instituto de Física Teórica, Universidade Estadual Paulista, São Paulo, Brazil*
[6]*Simon Fraser University, Vancouver, British Columbia, and York University, Toronto, Ontario, Canada*
[7]*University of Science and Technology of China, Hefei, People's Republic of China*
[8]*Universidad de los Andes, Bogotá, Colombia*
[9]*Charles University, Faculty of Mathematics and Physics, Center for Particle Physics, Prague, Czech Republic*
[10]*Czech Technical University in Prague, Prague, Czech Republic*
[11]*Center for Particle Physics, Institute of Physics, Academy of Sciences of the Czech Republic, Prague, Czech Republic*
[12]*Universidad San Francisco de Quito, Quito, Ecuador*
[13]*LPC, Université Blaise Pascal, CNRS/IN2P3, Clermont, France*
[14]*LPSC, Université Joseph Fourier Grenoble 1, CNRS/IN2P3, Institut National Polytechnique de Grenoble, Grenoble, France*
[15]*CPPM, Aix-Marseille Université, CNRS/IN2P3, Marseille, France*
[16]*LAL, Université Paris-Sud, CNRS/IN2P3, Orsay, France*
[17]*LPNHE, Universités Paris VI and VII, CNRS/IN2P3, Paris, France*
[18]*CEA, Irfu, SPP, Saclay, France*
[19]*IPHC, Université de Strasbourg, CNRS/IN2P3, Strasbourg, France*
[20]*IPNL, Université Lyon 1, CNRS/IN2P3, Villeurbanne, France and Université de Lyon, Lyon, France*
[21]*III. Physikalisches Institut A, RWTH Aachen University, Aachen, Germany*
[22]*Physikalisches Institut, Universität Freiburg, Freiburg, Germany*
[23]*II. Physikalisches Institut, Georg-August-Universität Göttingen, Göttingen, Germany*
[24]*Institut für Physik, Universität Mainz, Mainz, Germany*
[25]*Ludwig-Maximilians-Universität München, München, Germany*
[26]*Fachbereich Physik, Bergische Universität Wuppertal, Wuppertal, Germany*
[27]*Panjab University, Chandigarh, India*
[28]*Delhi University, Delhi, India*
[29]*Tata Institute of Fundamental Research, Mumbai, India*
[30]*University College Dublin, Dublin, Ireland*
[31]*Korea Detector Laboratory, Korea University, Seoul, Korea*
[32]*CINVESTAV, Mexico City, Mexico*
[33]*FOM-Institute NIKHEF and University of Amsterdam/NIKHEF, Amsterdam, The Netherlands*
[34]*Radboud University Nijmegen/NIKHEF, Nijmegen, The Netherlands*
[35]*Joint Institute for Nuclear Research, Dubna, Russia*
[36]*Institute for Theoretical and Experimental Physics, Moscow, Russia*
[37]*Moscow State University, Moscow, Russia*
[38]*Institute for High Energy Physics, Protvino, Russia*
[39]*Petersburg Nuclear Physics Institute, St. Petersburg, Russia*
[40]*Stockholm University, Stockholm and Uppsala University, Uppsala, Sweden*
[41]*Lancaster University, Lancaster LA1 4YB, United Kingdom*
[42]*Imperial College London, London SW7 2AZ, United Kingdom*
[43]*The University of Manchester, Manchester M13 9PL, United Kingdom*
[44]*University of Arizona, Tucson, Arizona 85721, USA*
[45]*University of California Riverside, Riverside, California 92521, USA*
[46]*Florida State University, Tallahassee, Florida 32306, USA*
[47]*Fermi National Accelerator Laboratory, Batavia, Illinois 60510, USA*
[48]*University of Illinois at Chicago, Chicago, Illinois 60607, USA*
[49]*Northern Illinois University, DeKalb, Illinois 60115, USA*
[50]*Northwestern University, Evanston, Illinois 60208, USA*

[51]*Indiana University, Bloomington, Indiana 47405, USA*
[52]*Purdue University Calumet, Hammond, Indiana 46323, USA*
[53]*University of Notre Dame, Notre Dame, Indiana 46556, USA*
[54]*Iowa State University, Ames, Iowa 50011, USA*
[55]*University of Kansas, Lawrence, Kansas 66045, USA*
[56]*Kansas State University, Manhattan, Kansas 66506, USA*
[57]*Louisiana Tech University, Ruston, Louisiana 71272, USA*
[58]*Boston University, Boston, Massachusetts 02215, USA*
[59]*Northeastern University, Boston, Massachusetts 02115, USA*
[60]*University of Michigan, Ann Arbor, Michigan 48109, USA*
[61]*Michigan State University, East Lansing, Michigan 48824, USA*
[62]*University of Mississippi, University, Mississippi 38677, USA*
[63]*University of Nebraska, Lincoln, Nebraska 68588, USA*
[64]*Rutgers University, Piscataway, New Jersey 08855, USA*
[65]*Princeton University, Princeton, New Jersey 08544, USA*
[66]*State University of New York, Buffalo, New York 14260, USA*
[67]*Columbia University, New York, New York 10027, USA*
[68]*University of Rochester, Rochester, New York 14627, USA*
[69]*State University of New York, Stony Brook, New York 11794, USA*
[70]*Brookhaven National Laboratory, Upton, New York 11973, USA*
[71]*Langston University, Langston, Oklahoma 73050, USA*
[72]*University of Oklahoma, Norman, Oklahoma 73019, USA*
[73]*Oklahoma State University, Stillwater, Oklahoma 74078, USA*
[74]*Brown University, Providence, Rhode Island 02912, USA*
[75]*University of Texas, Arlington, Texas 76019, USA*
[76]*Southern Methodist University, Dallas, Texas 75275, USA*
[77]*Rice University, Houston, Texas 77005, USA*
[78]*University of Virginia, Charlottesville, Virginia 22901, USA*
[79]*University of Washington, Seattle, Washington 98195, USA*

(Received 1 November 2010; published 28 February 2011)

The ratio of the cross section for $p\bar{p}$ interactions producing a Z boson and at least one b-quark jet to the inclusive $Z +$ jet cross section is measured using 4.2 fb^{-1} of $p\bar{p}$ collisions collected with the D0 detector at the Fermilab Tevatron collider at $\sqrt{s} = 1.96$ TeV. The $Z \to \ell^+\ell^-$ candidate events with at least one b jet are discriminated from $Z +$ charm and light jet(s) events by a novel technique that exploits the properties of the tracks associated to the jet. The measured ratio is 0.0193 ± 0.0027 for events having a jet with transverse momentum $p_T > 20$ GeV and pseudorapidity $|\eta| \leq 2.5$, which is the most precise to date and is consistent with theoretical predictions.

DOI: 10.1103/PhysRevD.83.031105 PACS numbers: 12.38.Qk, 13.85.Qk, 14.65.Fy, 14.70.Hp

The measurement of the production cross section for a Z boson in association with b jets provides an important test of perturbative quantum chromodynamics (QCD) predictions [1]. A good description of this process by theoretical calculations is essential since it is a major background to searches for the standard model (SM) Higgs boson via $ZH(H \to b\bar{b})$ associated production [2] and for the supersymmetric partners of b quarks [3]. This process is also sensitive to the b-quark density in the proton needed to predict phenomena such as single top quark production [4] and production of non-SM Higgs bosons in association with b quarks [5]. Calculations for the Z boson production in association with b quarks in $p\bar{p}$ collisions are available at next-to-leading order (NLO) using two different approaches [1,6], and they agree within their respective theoretical uncertainties.

In this paper, we describe a measurement of the ratio of the inclusive cross sections for Z boson production with at least one b-quark jet to the $Z +$ jet(s) production in $p\bar{p}$ interactions, where the Z boson is identified via its $Z \to ee$ and $Z \to \mu\mu$ decay modes. The $Z + b$ jet events are separated from Z boson production with light (u, d, or s quarks, or gluons) and charm (c) jet(s) by a discriminant that exploits the properties of the tracks associated to the

---

[*] Visitor from Augustana College, Sioux Falls, SD, USA.
[†] Visitor from The University of Liverpool, Liverpool, United Kingdom.
[‡] Visitor from SLAC, Menlo Park, CA, USA.
[§] Visitor from ICREA/IFAE, Barcelona, Spain.
[‖] Visitor from Centro de Investigacion en Computacion-IPN, Mexico City, Mexico.
[¶] Visitor from ECFM, Universidad Autonoma de Sinaloa, Culiacán, Mexico.
[**] Visitor from Universität Bern, Bern, Switzerland.

jet. The measurement of the ratio benefits from cancellations of many systematic uncertainties on the cross sections and therefore allows a more precise comparison with theoretical calculations. Previous measurements by the D0 [7] and CDF [8] Collaborations agree with the SM predictions. Here, we present the most precise measurement of the ratio to date. This measurement is a significant improvement over the previous D0 result [7] which utilized 0.18 fb^{-1} of integrated luminosity and assumed the ratio of the $Z + b$ jet cross section to the $Z + c$ jet cross section from NLO calculations. This analysis uses a much larger data set and a substantially improved method to extract the different jet flavor fractions. This measurement is done on an expanded jet kinematic region ($|\eta| < 2.5$), hence extending the test of QCD predictions and matching the η coverage of the Tevatron's efforts in the Higgs and new phenomena searches.

We use data from $p\bar{p}$ collisions at a center-of-mass energy of 1.96 TeV collected by the D0 detector [9] at the Fermilab Tevatron between 2006 and 2009 and corresponding to an integrated luminosity of 4.2 fb^{-1}. The selected events are required to pass at least one of the single electron or single muon triggers. The efficiency of the triggers, as measured from the data, is close to 100% (78%) for the $Z \to ee$ ($Z \to \mu\mu$) final state.

This analysis relies on all components of the detector: tracking, calorimetry, and the muon system and the ability to identify detached vertices. The D0 detector consists of a central tracking system, comprising a silicon microstrip tracker and a central fiber tracker, both within a 2 T solenoidal magnet; a liquid argon and uranium calorimeter, divided into a central calorimeter and two end cap calorimeters; and a muon system, consisting of three layers of tracking detectors and scintillation trigger counters. The silicon microstrip tracker allows a precise reconstruction of the $p\bar{p}$ interaction vertex (PV) and of eventual secondary vertices (SV) and an accurate determination of the impact parameter of a track relative to the PV, which are the key components of the jet lifetime based b-tagging algorithms. Offline event selection requires a reconstructed PV that has at least three associated tracks and is located within 60 cm of the center of the detector in the coordinate along the beam direction. The selected events must contain a Z boson candidate with a dilepton invariant mass $70\text{ GeV} < m_{\ell\ell} < 110\text{ GeV}$. Throughout this paper we use Z boson to denote any dilepton event in the above-mentioned mass range due to Z or γ^* production. The dielectron (ee) selection requires at least two electrons of transverse momentum $p_T > 15$ GeV identified by electromagnetic showers in the central (with pseudorapidity [10] $|\eta| < 1.1$) or end cap ($1.5 < |\eta| < 2.5$) calorimeter. The showers must have a significant fraction of their energy deposited in the electromagnetic calorimeter, be isolated from other energy depositions, and have a shape consistent with that expected for an electron. The central electrons, in addition, must match central tracks or produce electronlike patterns of hits in the tracker. The dimuon ($\mu\mu$) selection requires at least two muons with segments in the muon spectrometer matched to central tracks with $p_T > 10$ GeV and $|\eta| < 2$. Combined tracking and calorimeter isolation requirements are applied to the muon candidates. Muons from cosmic rays are rejected by applying a timing criterion to the hits in the scintillator layers as well as restricting the position of the muon track with respect to the PV. The two muons must also have opposite electric charges. A total of 411 064 (224 814) Z boson candidate events are retained in the ee ($\mu\mu$) channel. The $Z +$ jet sample is then selected by requiring the presence of at least one reconstructed jet with $|\eta| < 2.5$, with the leading jet having $p_T > 20$ GeV and any additional jets having $p_T > 15$ GeV. Jets are reconstructed from energy deposits in the calorimeter using the iterative midpoint cone algorithm [11] with a cone of radius 0.5. The energy of jets is corrected for detector response, the presence of noise, and multiple $p\bar{p}$ interactions, and the energy deposited outside of the jet cone used for reconstruction. Events with missing transverse energy larger than 60 GeV are rejected to suppress the background from $t\bar{t}$ production. These selection criteria yield a sample of 48 956 (24 450) $Z +$ jet events in the ee ($\mu\mu$) channel. Jets considered for b tagging are subject to a preselection, called taggability, to decouple the intrinsic b jet tagging algorithm performance from other effects. For this purpose, the jet is required to have at least two associated tracks with $p_T > 0.5$ GeV, the leading track must have $p_T > 1.0$ GeV, and each track must have at least one silicon microstrip tracker hit. This requirement has a typical efficiency of 90% per jet. The jet related efficiencies mentioned here and later on are determined from simulations and corrected for the difference observed in the data. In order to enrich a sample with heavy-flavor jets, a neural network (NN) based b-tagging algorithm is applied that exploits the longer lifetimes of b-flavored hadrons in comparison to their lighter counterparts [12]. The inputs to the NN combine several characteristic quantities of the jet and associated tracks to provide a continuous output value that tends towards one for b jets and zero for non-b jets. The important input variables are the number of reconstructed SV in the jet, the invariant mass of charged particles associated with the SV (M_{SV}), the number of tracks used to reconstruct the SV, the two-dimensional decay length significance of the SV in the plane transverse to the beam, a weighted combination of the tracks' transverse impact parameter significances, and the probability that the tracks from the jet originate from the PV, which is referred to as the jet lifetime probability (JLIP). We require at least one of the jets in the event to have a NN output greater than 0.5. In about 10% of the events the leading jet is not tagged. In this case we apply the NN selection to subleading jets. A total of 2200 (1015) events with at least one b tagged jet candidate are thus selected in the ee ($\mu\mu$) channel. The tagging efficiency for b jets and the mistagging rate of light jets are parametrized as functions of jet p_T and η and are about 58% and 2%, respectively, averaged over the kinematics of jets considered in this analysis. Jets containing b quarks have a different energy response and receive an average additional energy correction of 6% as determined from simulations. To further separate b jets from c and light jets, we construct a discriminant ($D_{\rm JLIP}^{M_{\rm SV}}$) from the combination of $M_{\rm SV}$ and JLIP, $D_{\rm JLIP}^{M_{\rm SV}} \equiv (M_{\rm SV}/10\ {\rm GeV} - \ln({\rm JLIP})/40)$. The relative weights of the variables are selected based on studies of simulated data to maximize rejection of c and light quark jets. The mass $M_{\rm SV}$ provides good discrimination between b, c, and light jets due to the different masses of the quarks. Jets from b quarks usually have large values of $-\ln({\rm JLIP})$, while light jets mostly have small values, as their tracks originate from the PV. The average efficiency for the b jets in the data to have a well-defined $D_{\rm JLIP}^{M_{\rm SV}}$ output is about 68%, which is due to the finite efficiency for a b jet to have a reconstructed SV. Figure 1 shows the normalized distributions of $D_{\rm JLIP}^{M_{\rm SV}}$ for jets of different flavors after the NN b tagging requirement. The discriminant $D_{\rm JLIP}^{M_{\rm SV}}$ separates well between b, c, and light jets. Figure 1 also shows the $D_{\rm JLIP}^{M_{\rm SV}}$ distribution of the tagged jets derived from a light jet enriched data sample, referred to as negatively tagged (NT) data. NT jets have negative values for some of the inputs for the NN algorithm [12] such as decay length significance and impact parameter which are caused by the detector resolution effects. We estimate the b jet contamination in the NT data using a maximum likelihood fit and subtract its contribution. The template shapes in the corrected NT data and the light jets in the Monte Carlo (MC) simulation look similar and the small difference is taken as a systematic uncertainty.

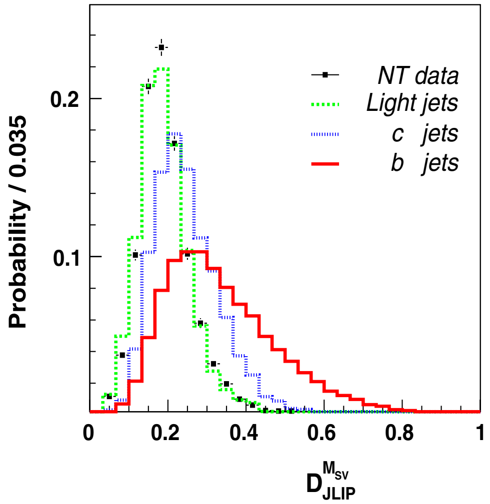

FIG. 1 (color online). The probability densities of the $D_{\rm JLIP}^{M_{\rm SV}}$ discriminant for b, c, and light jets passing the NN b tagging requirement. Also shown is the distribution for the negative tagged (NT) jets in the data, described in the text.

The dominant background to Z + jet production arises from multijet (MJ) events in which jets are misreconstructed as leptons, especially in the ee channel. This instrumental background is estimated from the data. We use MJ-enriched data samples that pass all event selection requirements, but fail some of the lepton quality criteria, to determine the kinematic shape of the background distribution. For the ee channel, the MJ sample is obtained by inverting the shower shape requirements and relaxing other identification criteria on the electron candidates. For the $\mu\mu$ channel, the MJ sample consists of events with muon candidates that fail the isolation criteria. Smaller background contributions arise from top quark pair ($t\bar{t}$) and diboson (WW, WZ, ZZ) production, which contain two leptons in the final state. These backgrounds are estimated using MC simulations with the cross sections rescaled to match theoretical calculations [13,14]. We simulate inclusive diboson production with PYTHIA [15]. Events from Z + jet and $t\bar{t}$ processes are generated with ALPGEN [16], interfaced with PYTHIA for initial and final state radiation and for hadronization. For these events, a matching procedure is used to avoid double counting of partons produced by ALPGEN and those subsequently added by the showering in PYTHIA. The Z + jets samples consist of Z + light jets and a Z + heavy-flavor component, which includes $Z + b\bar{b}(c\bar{c})$ production. All simulations use the CTEQ6L1 [17] parton distribution functions. All samples are processed using a detector simulation based on GEANT3 [18] and the same offline reconstruction algorithms as for the data. Events from randomly chosen beam crossings are overlaid on the simulated events to reproduce the effect of multiple $p\bar{p}$ interactions and detector noise. The normalizations of the simulated and the MJ backgrounds are adjusted by scale factors determined from a fit to the $m_{\ell\ell}$ distributions in the inclusive untagged sample. The background fraction in the ee channel is about 18% for both the inclusive untagged and tagged samples and is dominated by the MJ background. The $\mu\mu$ channel has a higher purity, with a background fraction of only about 0.8% in the untagged and tagged samples. Corrections are applied to the simulated events to improve the MC modeling. The simulated $Z \to \mu\mu$ events are weighted with trigger efficiencies measured in the data. For the ee channel, no correction is applied as the corresponding trigger is nearly 100% efficient. Lepton identification efficiencies are corrected as a function of η, azimuthal angle ϕ, and the z position of the PV. Jet energies are smeared to reproduce the resolution observed in the data, and the efficiency for reconstructing a jet is corrected to match the one in the data. The simulated Z boson events are reweighted such that the p_T distribution of the Z boson is consistent with the observed distribution. Figures 2(a) and 2(b) show the p_T distribution of the leading jet in the data compared with the expectation from simulation for Z + jets inclusive events and the associated contributions in each channel.

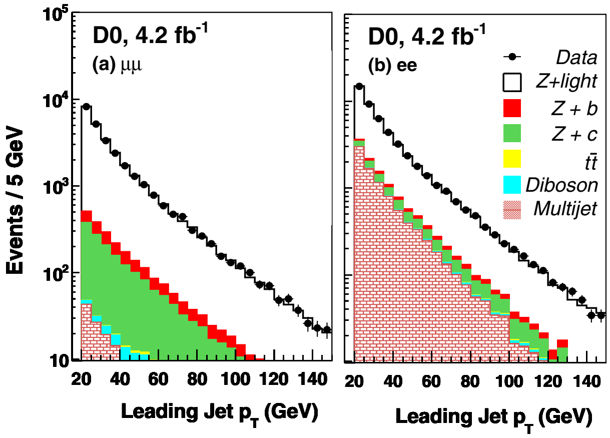

FIG. 2 (color online). The observed p_T distribution of the leading jet in the (a) $\mu\mu$ and (b) ee channel compared with the SM prediction. The uncertainties on the data points are statistical, and the prediction is normalized to the data, as described in the text.

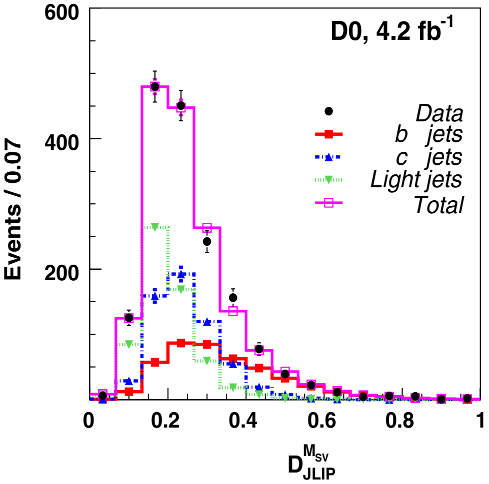

FIG. 3 (color online). The $D_{\rm JLIP}^{M_{\rm SV}}$ discriminant distribution of events in the combined sample. The distributions of the b, c, and light jets are weighted by the fractions found from the fit. Uncertainties are statistical only.

The dominant contribution comes from Z + light jet production. In order to measure the fraction of events with different jet flavors in the final selected sample, we perform a binned maximum likelihood fit to the $D_{\rm JLIP}^{M_{\rm SV}}$ distribution in the data using a combination of the light, c, and b flavor jet templates. Before the fit, we subtract the non-(Z + jet) background contributions. A total of 970 (630) events remains in the ee ($\mu\mu$) channel passing all selection requirements and after the background subtraction. The b and c jet $D_{\rm JLIP}^{M_{\rm SV}}$ templates are taken from MC simulations with correction factors applied to account for the differences in the data and MC efficiencies. The light jet template is obtained from the higher statistics NT data described earlier. The jet flavor fractions obtained in the ee and $\mu\mu$ channels are shown in Table I, where the uncertainties are from the fit due to the data and template statistics. The relative light and c-quark fractions are not tightly constrained by the data. The b jet fraction is, however, largely insensitive to variations in the relative amount of light and c jets. Since the individual samples yield consistent results, we combine the ee and $\mu\mu$ samples and remeasure the fractions using an independent fit. The $D_{\rm JLIP}^{M_{\rm SV}}$ distributions in the two data samples used for fitting agree after background subtraction. The last column of Table I gives the results of the jet flavor fractions from the combined sample. Figure 3 shows the combined $D_{\rm JLIP}^{M_{\rm SV}}$ distribution of b-tagged jets for data along with the fitted contributions from the light (NT data), c, and b jets. The extracted jet flavor fractions are used to determine the ratio $\sigma(Z + b{\rm jet})/\sigma(Z + {\rm jet})$ as follows:

$$\frac{\sigma(Z + b\ {\rm jet})}{\sigma(Z + {\rm jet})} = \frac{N_b}{N_{\rm incl}\epsilon_b^{\rm tag}\epsilon_{b/{\rm incl}}^{\rm reco}}, \tag{1}$$

where $N_{\rm incl}$ is the total number of Z + jet events before any tagging requirement, N_b is the number of $Z + b$ jet events obtained from the $D_{\rm JLIP}^{M_{\rm SV}}$ fit, $\epsilon_b^{\rm tag}$ is the overall $D_{\rm JLIP}^{M_{\rm SV}}$ efficiency for b jets, which combines the efficiencies for taggability, NN tagger, and $D_{\rm JLIP}^{M_{\rm SV}}$ selection, and $\epsilon_{b/{\rm incl}}^{\rm reco}$ accounts for the difference between b and inclusive jet reconstruction efficiencies. Several experimental uncertainties cancel out in the measurement of $\sigma(Z + b{\rm jet})/\sigma(Z + {\rm jet})$, including the uncertainties on the luminosity and trigger, lepton, and some jet identification efficiencies. The two largest remaining sources of systematic uncertainty are uncertainties in the $D_{\rm JLIP}^{M_{\rm SV}}$ efficiency and in the shape of the $D_{\rm JLIP}^{M_{\rm SV}}$ templates used for the extraction of the b jet fraction. Variation in $D_{\rm JLIP}^{M_{\rm SV}}$ efficiency by 1 standard deviation results in an uncertainty of 3.7% on the final result. The uncertainty due to the shape of the templates (4.2%) is estimated by using an alternate light jet template from MC, by changing the b-quark fragmentation function [15], and by varying the fraction of merged heavy quarks ($b\bar{b}$, $c\bar{c}$) inside the jet. An additional uncertainty on the c jet template shape has been evaluated by varying the D^+/D^0 ratio by 20% which yields a negligible contribution of less than 1% to the systematic uncertainty. Other important sources of uncertainty are the b tagging efficiency (2.4%), the b jet energy scale (2%), and reconstruction efficiency (3.2%). The total systematic

TABLE I. Jet flavor fractions obtained from template fitting in the dielectron, dimuon, and combined channels, along with statistical uncertainties.

Channel	$\mu\mu$	ee	Combined
Events	630	970	1600
$Z + b$	0.248 ± 0.042	0.267 ± 0.036	0.259 ± 0.028
$Z + c$	0.253 ± 0.073	0.364 ± 0.064	0.359 ± 0.049
Z + light	0.499 ± 0.058	0.369 ± 0.049	0.382 ± 0.038

uncertainty on the measurement of the ratio is 7.7%. The final result is

$$\frac{\sigma(Z + b\ \mathrm{jet})}{\sigma(Z + \mathrm{jet})} = 0.0193 \pm 0.0022(\mathrm{stat}) \pm 0.0015(\mathrm{syst}), \tag{2}$$

which is consistent with the ratios obtained separately for the two channels. This measurement is the most precise to date. For the kinematic region considered in the analysis, an NLO MCFM [1] prediction for the ratio yields 0.0192 ± 0.0022; this is obtained for the renormalization and factorization scales $Q_R^2 = Q_F^2 = m_Z^2$ (m_Z being the Z boson mass) and with the Martin-Stirling-Thorne-Watt 2008 parton distribution functions [19]. The prediction decreases by 3.6% when the effects from detector response and resolution as well as hadronization and underlying event are taken into account.

In summary, we have performed the most precise measurement to date of the ratio of the cross section for Z boson production in association with at least one b jet to the inclusive Z + jet cross section, considering final states with $Z \to ee$ and $Z \to \mu\mu$ and jets with $p_T > 20$ GeV and $|\eta| \leq 2.5$. The combined measurement of the ratio yields 0.0193 ± 0.0027, which is consistent with NLO QCD calculations. This measurement allows precision tests of QCD in a much larger rapidity region that matches, e.g., the Tevatron's efforts in Higgs particle searches.

We thank the staffs at Fermilab and collaborating institutions and acknowledge support from the DOE and NSF (USA); CEA and CNRS/IN2P3 (France); FASI, Rosatom, and RFBR (Russia); CNPq, FAPERJ, FAPESP, and FUNDUNESP (Brazil); DAE and DST (India); Colciencias (Colombia); CONACyT (Mexico); KRF and KOSEF (Korea); CONICET and UBACyT (Argentina); FOM (The Netherlands); STFC and the Royal Society (United Kingdom); MSMT and GACR (Czech Republic); CRC Program and NSERC (Canada); BMBF and DFG (Germany); SFI (Ireland); The Swedish Research Council (Sweden); and CAS and CNSF (China). We thank the author of MCFM for the help with useful discussion on the theoretical calculations.

[1] J. M. Campbell, R. K. Ellis, F. Maltoni, and S. Willenbrock, Phys. Rev. D **69**, 074021 (2004).

[2] V. M. Abazov *et al.* (D0 Collaboration), Phys. Rev. Lett. **104**, 071801 (2010); **105**, 251801 (2010); T. Aaltonen *et al.* (CDF Collaboration), Phys. Rev. D **80**, 071101 (2009); Phys. Rev. Lett. **105**, 251802 (2010).

[3] V. M. Abazov *et al.* (D0 Collaboration), Phys. Lett. B **693**, 95 (2010); T. Aaltonen *et al.* (CDF Collaboration), Phys. Rev. Lett. **105**, 081802 (2010).

[4] V. M. Abazov *et al.* (D0 Collaboration), Phys. Rev. Lett. **103**, 092001 (2009); T. Aaltonen *et al.* (CDF Collaboration), Phys. Rev. Lett. **103**, 092002 (2009).

[5] T. Affolder *et al.* (CDF Collaboration), Phys. Rev. Lett. **86**, 4472 (2001); V. M. Abazov *et al.* (D0 Collaboration), Phys. Rev. Lett. **95**, 151801 (2005); **101**, 221802 (2008).

[6] F. F. Cordero, L. Reina, and D. Wackeroth, Phys. Rev. D **78**, 074014 (2008).

[7] V. M. Abazov *et al.* (D0 Collaboration), Phys. Rev. Lett. **94**, 161801 (2005).

[8] A. Abulencia *et al.* (CDF Collaboration), Phys. Rev. D **74**, 032008 (2006); T. Aaltonen *et al.* (CDF Collaboration), Phys. Rev. D **79**, 052008 (2009).

[9] V. M. Abazov *et al.* (D0 Collaboration), Nucl. Instrum. Methods Phys. Res., Sect. A **565**, 463 (2006); M. Abolins *et al.*, Nucl. Instrum. Methods Phys. Res., Sect. A **584**, 75 (2008); R. Angstadt *et al.*, Nucl. Instrum. Methods Phys. Res., Sect. A **622**, 298 (2010).

[10] Pseudorapidity $\eta = -\ln[\tan(\theta/2)]$ with polar angle θ measured relative to the proton beam direction.

[11] G. C. Blazey *et al.*, arXiv:hep-ex/0005012.

[12] V. M. Abazov *et al.* (D0 Collaboration), Nucl. Instrum. Methods Phys. Res., Sect. A **620**, 490 (2010).

[13] N. Kidonakis and R. Vogt, Phys. Rev. D **78**, 074005 (2008).

[14] J. M. Campbell and R. K. Ellis, Phys. Rev. D **60**, 113006 (1999).

[15] T. Sjöstrand, S. Mrenna, and P. Skands, J. High Energy Phys. 05 (2006) 026. Version 6.409 with Tune A is used.

[16] M. L. Mangano *et al.*, J. High Energy Phys. 07 (2003) 001. Version 2.11 is used.

[17] J. Pumplin *et al.*, J. High Energy Phys. 07 (2002) 012.

[18] R. Brun and F. Carminati, CERN Program Library Long Writeup Report No. W5013, 1993.

[19] A. D. Martin, W. J. Stirling, R. S. Thorne, and G. Watt, Eur. Phys. J. C **63**, 189 (2009).